CORE
Metadata, citation and similar papers at core.ac.uk
Provided by Greenwich Academic Literature Archive

Multi-Mode Resonator-Fed Dual Polarized Antenna Array with Enhanced Bandwidth and Selectivity

Chun-Xu Mao, Steven Gao, Member, IEEE, Yi Wang, Senior Member, IEEE, Fan Qin, Qing-Xin Chu, Senior Member, IEEE

Abstract— A novel design concept of multi-mode filtering antenna, which is realized by integrating a multi-mode resonator and an antenna, has been applied to the design of dual-polarized antenna arrays for achieving a compact size and high performance in terms of broad bandwidth, high frequency selectivity and out-of-band rejection. To verify the concept, a 2×2 array at C-band is designed and fabricated. The stub-loaded resonator (SLR) is employed as the feed of the antenna. The resonant characteristics of SLR and patch as well as the coupling between them are presented. The method of designing the integrated resonator-patch module is explained. This integrated design not only removes the need for separated filters and traditional 50 Ω interfaces, but also improves the frequency response of the module. A comparison with the traditional patch array has been made, showing that the proposed design has a more compact size, wider bandwidth, better frequency selectivity and out-of-band rejection. Such low-profile light weigh broadband dual polarized arrays are useful for space-borne synthetic aperture radar (SAR) and wireless communication applications. The simulated and measured results agree well, demonstrating a good performance in terms of impedance bandwidth, frequency selectivity, isolation, radiation pattern and antenna gain.

Index Terms— Antenna array, broadband, dual-polarization, filtering antenna, synthetic aperture radar (SAR), stub-loaded resonator (SLR).

I. INTRODUCTION

RECENTLY, space-borne synthetic aperture radar (SAR) has become increasing important for earth observation due to its capacity of operation under all weather conditions day and night. As a key component of the space-borne SAR system, the antenna is required to have compact size, light weight, low cost, low profile, broad bandwidth and high frequency selectivity. Such antennas are also required in terrestrial wireless communication and satellite communications. In [1]-[3], dual-band or triple-band shared aperture arrays were proposed to reduce the volume and weight of SAR system. Broad antennas are often realized by adopting stacked parasitic patches with a large air gap between them [1]-[10]. An H-shaped slot in the ground plane can also increase the bandwidth at the expense of higher backward radiation [11], [12]. An L-probe feeding has also been used to compensate the inductance of the patch, so as to improve its bandwidth [13]. These methods can be employed to design broadband antennas with a bandwidth over 20 % at the expense of a large thickness and complex structure of the antenna.

To improve the signal quality and reduce the interferences from the out-of-bands, band-pass filters are required in the RF front-end systems. Usually, the filter and the antenna are cascaded, which not only increases the volume, but also degrades the frequency response due to the mismatch and extra insertion loss caused by the interconnections between them. To reduce the size of RF front end and achieve high performance of broad bandwidth and higher frequency selectivity, it is necessary to employ seamless integration of the filter and the antenna and eliminate the interface between them [14], [15].

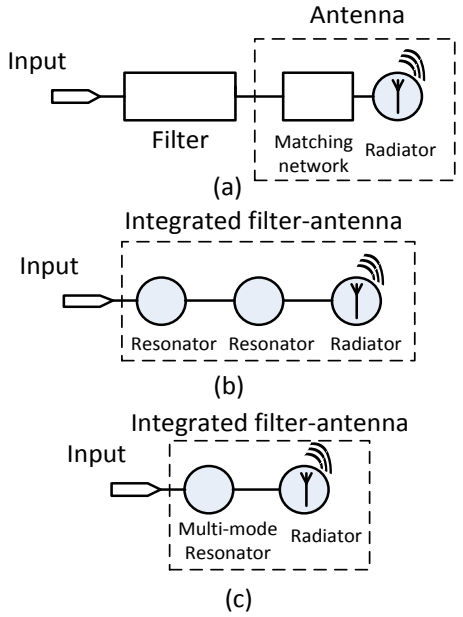

Fig. 1 The RF front-end subsystem: (a) traditional architecture, (b) single-mode resonator feeding, (c) proposed dual-mode resonator feeding.

This manuscript is submitted on March 20, 2015. This work is supported by the project "DIFFERENT" funded by EC FP7 (grant no. 6069923). YW is supported by UK EPSRC under Contract EP/M013529/1.

C. X. Mao, S. Gao and F. Qin are with the School of Engineering and Digital Arts, University of Kent, UK. (e-mail: cm688@kent.ac.uk, s. gao@kent.ac.uk).

Y. Wang is with the Department of Engineering Science, University of Greenwich, UK. (e-mail: yi.wang@greenwich.ac.uk).

Q. X. Chu with South China University of Technology, China (e-mail: qxchu@scut.edu.cn).

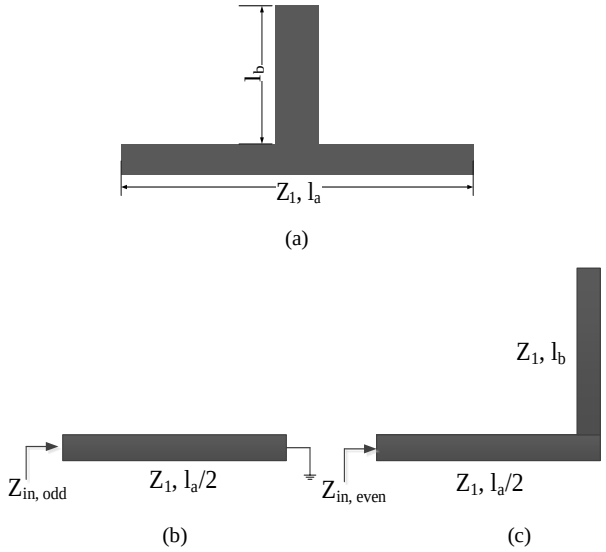

Fig.2 SLR and its equivalent circuit: (a) geometry, (b) odd-mode equivalent, (c) even-mode equivalent.

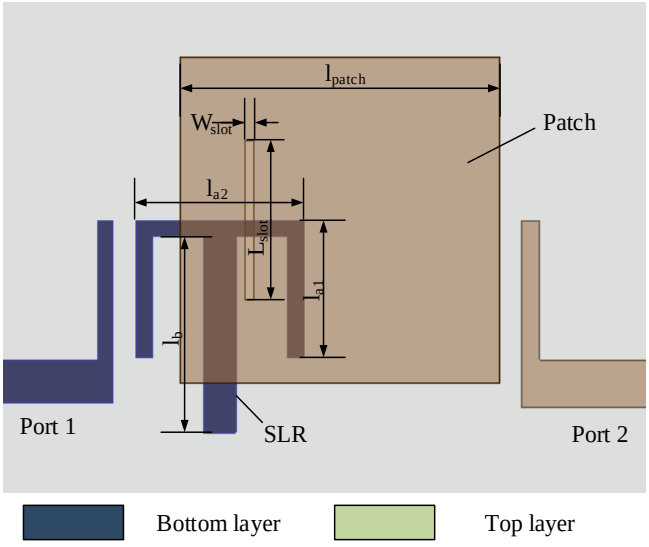

Fig. 3 The configuration of a SLR-patch bandpass filter. The coupling slot is cut in the ground plane, a layer between the top and bottom layer.

In this paper, a novel design method is proposed by using the stub loaded resonator (SLR) as the feed of the antenna. The odd- and even-mode of the SLR and the patch as a resonator are studied to realize a broadband antenna with a low profile. The coupling between the SLR and the patch is investigated to control the bandwidth. To verify this design concept, a 2×2 antenna array is designed, fabricated and measured for space-borne SAR applications. To better illustrate the merits of this novel integrated design, a traditional cascaded filter-antenna subsystem is also built for comparison. The results demonstrate that the integrated design has much improved performance in terms of broadband impedance matching, high frequency selectivity, ports isolation, antenna gains, cross polarization discrimination (XPD) and radiation efficiency.

This paper is organized as follow. Section II introduces the front-end systems evolution and proposed design methodology. Section III presents antenna design of dual polarized SLR-fed antenna element and array. Section IV highlights the advantages of the integrated design over the traditional cascaded design through comparison. Section V presents the measured results followed by conclusion.

II. DESIGN METHODOLOGY

A. Evolution of the front-end

It is well known that the RF front-end of advanced wireless systems are required to have compact size, low cost and multiple functions. Fig. 1(a) presents the traditional architecture of a RF front-end, where the filter and antenna are designed separately and cascaded with 50 Ω interfaces and matching networks. Fig. 1(b) shows an integrated filtering antenna, where the separated matching network is eliminated and the filter and the antenna are integrated seamlessly. The antenna radiator serves as the last resonator of the filter and the resonators feed into the radiator through coupling. The single-mode resonators and the antenna radiator are synchronously tuned to generate an operating band equivalent to a three-pole filter.

To make the integrated filter-antenna system more compact, a multi-mode resonator-fed antenna is proposed in this paper, as shown in Fig. 1 (c). The multi-mode resonator is coupled with the antenna, effectively generating a multi-mode antenna with broad bandwidth and filtering performance.

B. Study of the SLR and patch

To demonstrate the design concept of Fig.1 (c), a stub loaded resonator (SLR) is adopted. As shown in Fig. 2 (a), the SLR is a dual-mode resonator with two independently controllable resonant modes. Due to the symmetric of the SLR, it can be analyzed using the odd- and even-mode method [16]. Fig. 2 (b) (c) present the equivalent circuits of the odd-mode and even-mode, respectively. When the odd-mode is excited, the voltage at the middle of the SLR is zero and the SLR is shorted there, as depicted in Fig. 2(b). When the even-mode is excited, the symmetrical plane can be viewed as a magnetic wall, equivalent to an open circuit, as depicted in Fig. 2(c). The input impedance of the odd-mode and even-mode can be derived as

$$Z_{in,odd} = jZ_1 \tan\beta(l_a/2) \quad (1)$$

$$Z_{in,even} = j\frac{Z_1}{\tan\beta(l_a/2+l_b)} \quad (2)$$

where Z_1 is the characteristic impedance of the horizontal microstrip line in Fig. 2(a), and β is the propagation constant. When the input impedance Z_{in} becomes infinite, the odd-mode and even-mode resonate. Their resonant frequencies are

$$f_{odd} = \frac{c}{2\times l_a \times \sqrt{\varepsilon_{eff}}} \quad (3)$$

$$f_{even} = \frac{c}{2\times (l_a/2+l_b)\times \sqrt{\varepsilon_{eff}}} \quad (4)$$

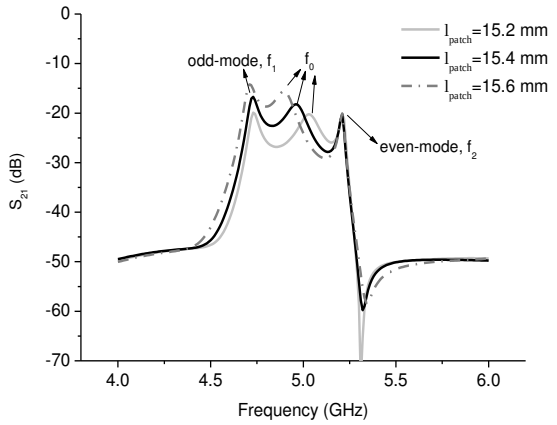

Fig. 4 The change of the resonant frequencies of the structure in Fig. 3 with l_{patch}.

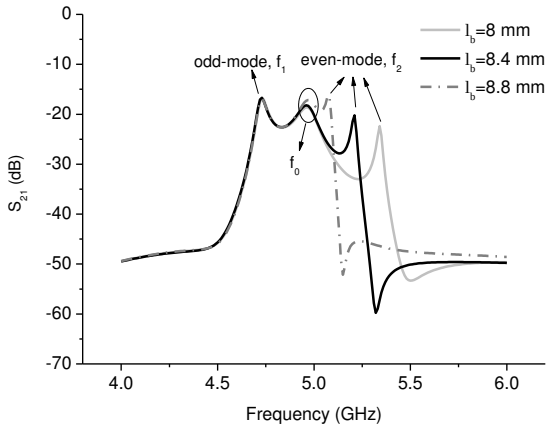

Fig. 6 The change of the resonant frequencies of the structure in Fig. 3 with l_b.

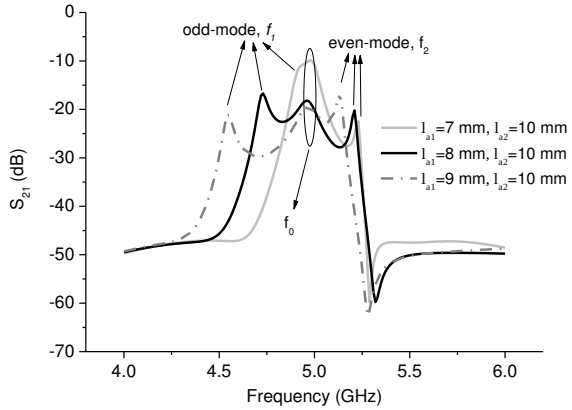

Fig. 5 The change of the resonant frequencies of the structure in Fig. 3 with l_{a1}.

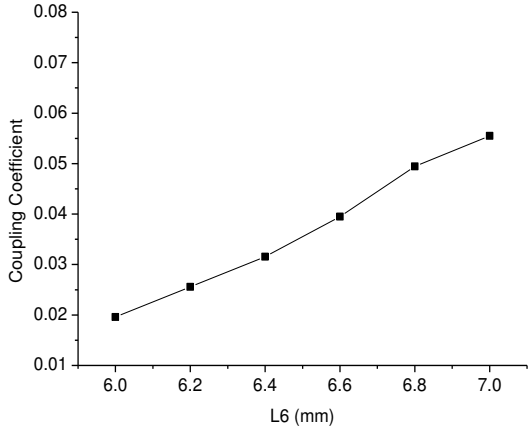

Fig. 7 The variation of the coupling coefficient with the length of the slot.

where, ε_{eff} is the effective dielectric constant, c is the speed of light. It is observed from (3) and (4) that the odd-mode and even-mode resonant frequencies can be controlled by tuning the lengths of the stubs.

To examine the coupling between the SLR and the patch, a two-port circuit composed of a SLR and a patch on different layers is constructed, as shown in Fig. 3. Rogers 4003 substrates with a dielectric constant of 3.55 and loss tangent of 0.0027 is used in the design. The SLR is printed on the bottom layer of the lower substrate with a thickness of 0.813 mm and the patch is printed on the top layer of the upper substrate with a thickness of 1.525 mm. The resonator in Fig. 2 is folded for compactness, as characterized by the two sections l_{a1} and l_{a2}, respectively in Fig. 3. The SLR is coupled with the patch through a slot in the ground plane with the dimension of l_{slot}=7 mm and w_{slot}=0.3 mm. The dimension of the square patch l_{patch} is about half wavelength at the operating frequency. By adjusting the coupling between the SLR and the patch, a pass band with three transmission modes can be obtained, as shown in Fig. 4. It is observed that the odd- and even-mode frequencies f_1 and f_2 of the SLR are located at both sides of the patch resonant frequency f_0. f_0 changes with the length of the patch l_{patch}.

Fig. 5 shows that the odd- and even-mode resonant frequencies vary with the total lengths of SLR l_a. It is observed that the influence on the odd-modes is more significant than that of the even-mode. Fig. 6 shows the resonant modes vary with the stub length l_b. It is observed that the even-mode resonant frequency f_2 shifts to lower frequency when l_b increases, whereas the f_0 and f_1 keep unchanged. Therefore, the three resonant frequencies can be controlled independently by tuning the dimensions of the patch and SLR. As a result, the bandwidth can be controlled.

The coupling strength between the SLR and the patch also has a significant influence on the bandwidth of the filtering antenna. The coupling can be controlled by the length and width of the slot in the ground. The coupling coefficient can be extracted using [17],

$$M_{ij} = \frac{f_j^2 - f_i^2}{f_j^2 + f_i^2} \qquad (5)$$

where f_i is the resonant frequency of the SLR and f_j is the resonant frequencies of the patch, respectively. Using full-wave

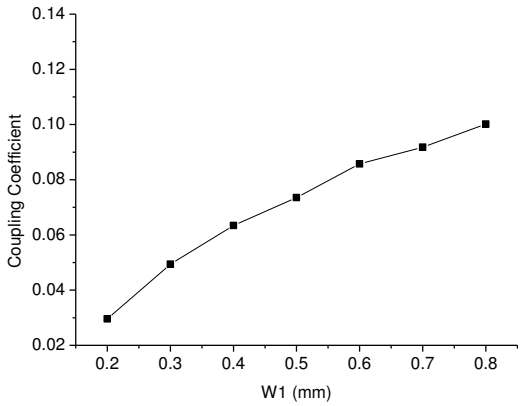

Fig. 8 The variation of the coupling coefficient with the width of the slot.

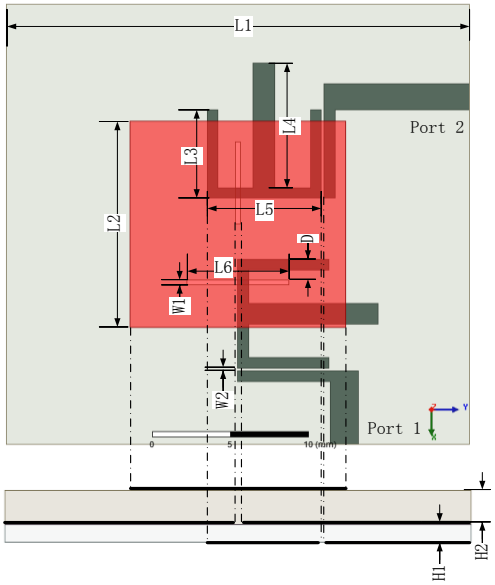

Fig. 9 The configuration of SLR-fed dual polarized antenna element.

Table 1: Parameters of the filtering antenna: (mm)

L1	L2	L3	L4	L5	L6
30	14	5.9	8.4	7.4	6.8
W1	W2	D	H1	H2	
0.3	0.2	1.4	0.813	1.525	

simulation, f_i and f_j can be obtained and the coupling coefficient can be calculated.

Fig. 7 shows that the simulated coupling coefficient between the SLR and patch varies with the lengths of the slot. It is observed that the coupling coefficient increases when the length increases. Similarly, when the width of the slot increases, a stronger coupling can also be observed, as depicted in Fig. 8. In this design, L6 = 6.8 mm and W1 = 0.3 mm are chosen.

III. DUAL-POLARIZED ANTENNA ARRAY DESIGN

A. SLR-fed antenna element

Fig. 9 shows the configuration of one dual-polarization integrated filtering-antenna element. The radiating element on the top layer is fed by the SLR in the bottom layer via the slot in the ground plane in the middle layer. The antenna and the feeding network are printed on two substrates of Rogers 4003 with the thickness of 1.525 mm and 0.813 mm, respectively. The two slots in the ground plane are placed perpendicular to each other to reduce the coupling between the two polarizations. Different from the traditional aperture coupled patch antenna using the microstrip line, the patch in this design is coupled to a resonator. The SLR in positioned in relative to the slot in such a way as to obtain strong magnetic coupling between them. In order to realize a wideband performance, the odd- and even-mode of the SLR are placed at both sides of the resonant frequency of the patch. The simulation were performed using High Frequency Simulation Software (HFSS) and the optimized parameters are presented in Table 1. It should be noted that the thickness of the whole module is 2.338 mm with two substrates, which is much lower than the previous work in the references [1]-[13].

For the SLR-fed antenna, the bandwidth can be controlled by

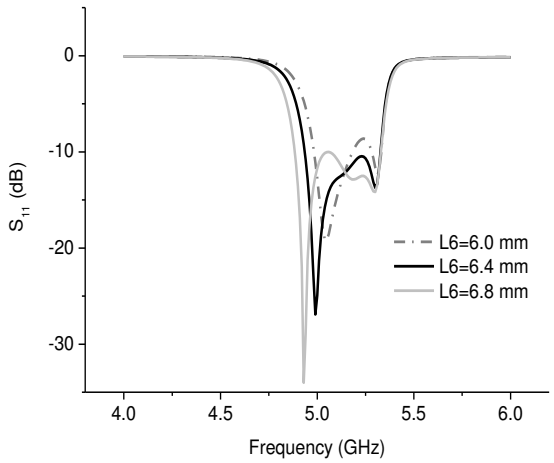

Fig. 10 The variation of the bandwidth with L6.

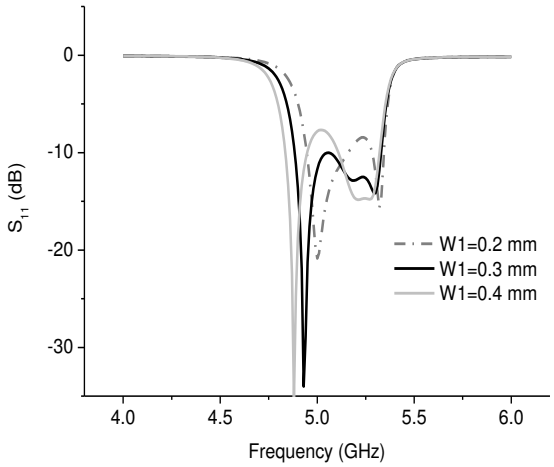

Fig. 11 The variation of the bandwidth with W1.

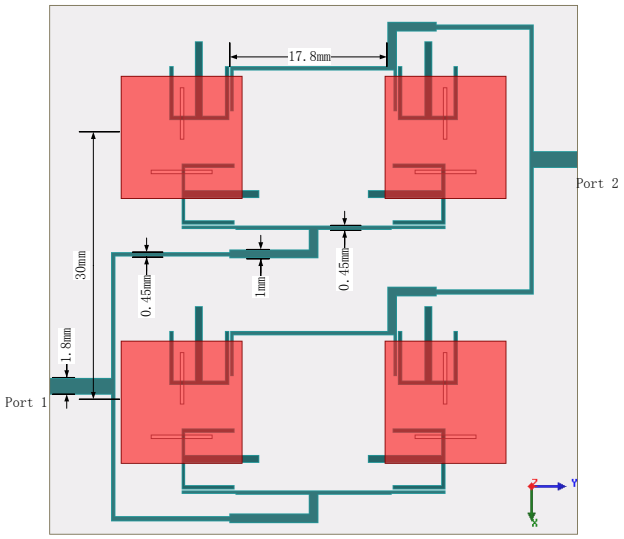

Fig. 12 The layout of the 2 × 2 SLR-fed dual polarization array.

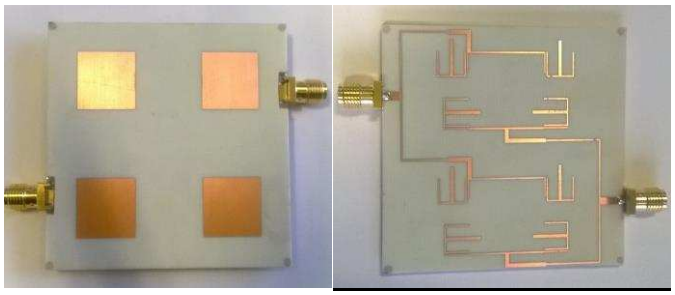

(a) (b)

Fig. 13 The prototype of the 2×2 dual polarization SLR-fed array: (a) top layer, (b) bottom layer.

tuning the dimension of the SLR or the coupling strength between the SLR and the patch. Fig. 10 shows that the bandwidth of the antenna vary with different lengths of the slot. It is observed that the first and the second resonant frequencies separate when L6 increases, resulting in a wider bandwidth. Similarly, when the width W1 increases, the coupling strength and bandwidth also increase, as shown in Fig. 11.

B. SLR-fed 2×2 dual-polarized array

Fig. 12 shows the layout of the 2×2 dual polarization antenna array fed by SLRs for the SAR applications. The array works in C-band with the central frequency of 5.2 GHz. The spacing between the elements is 30 mm (0.53 λ_0). For X-direction polarization (excitation from port 1), a four-way T-shaped power divider is used to feed the SLRs. For Y-direction polarization (excitation from port 2), an out-of-phase T-shaped power divider is adopted to feed the SLRs. The 180° phase difference is achieved by extending one branch of transmission lines by half of a guided wavelength (i.e. 17.8 mm). The out-of-phase power divider here is used to improve the cross polarization discrimination (XPD) [18]. Quarter-wavelength impedance transformer is used for impedance matching. The size of the 2×2 array is 60 mm ×60 mm with a thickness of 2.338 mm. Fig. 13 shows the top and bottom layers of the prototype array.

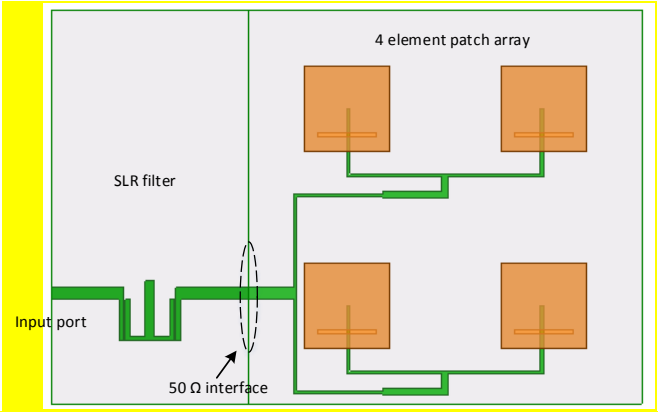

Fig. 14 Configuration of the conventional cascaded filter-antenna. Only one polarization is implemented.

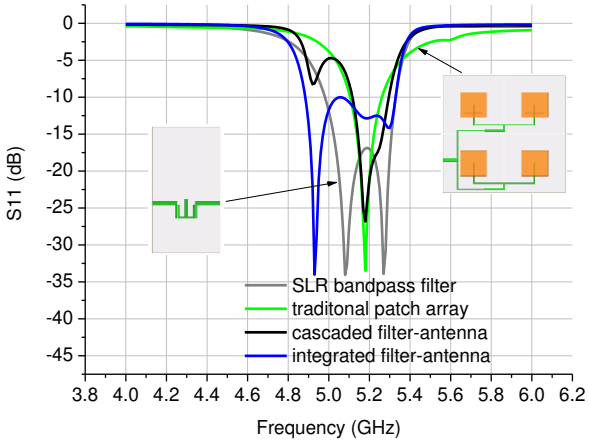

Fig. 15 The S11 comparison between four devices: the SLR filter, the parch array, the cascaded filter-antenna and the integrated filter-antenna.

IV. COMPARISON WITH CONVENTIONAL DESIGN

To better illustrate the merits of the integrated filter-antenna design, a traditional cascaded filter-antenna module is built and compared, as shown in Fig. 14. Without loss of generality, only one polarization is implemented. The bandpass filter and the patch array are designed independently and then cascaded with the 50 Ω interface. The bandpass filter is composed of the dual-mode SLR. The four-element patch array is directly fed by a T-shape four-way power divider via coupling slots. The input impedance of the antenna array is set as 50 Ω. Firstly, it is evident that the size of this cascaded structure is larger than the integrated structure in Fig. 12.

Fig. 15 compares the impedance bandwidth of the SLR filter, the standalone patch array, the cascaded filter-antenna and the integrated filter-antenna. As can be seen, the traditional patch array has a -10 dB bandwidth of only 150 MHz, mainly due to the narrowband nature of the patch. Fig. 15 also shows the standalone SLR filter has the 2nd order characteristics with two poles and a bandwidth of 350 MHz. For the cascaded module, the overall bandwidth is largely limited by the narrowband component which is the patch array in the design. This is evident shown from Fig. 15 that a bandwidth of only 170 MHz for the cascaded filter-antenna is achieved. This is much smaller than the integrated design, which exhibits a bandwidth

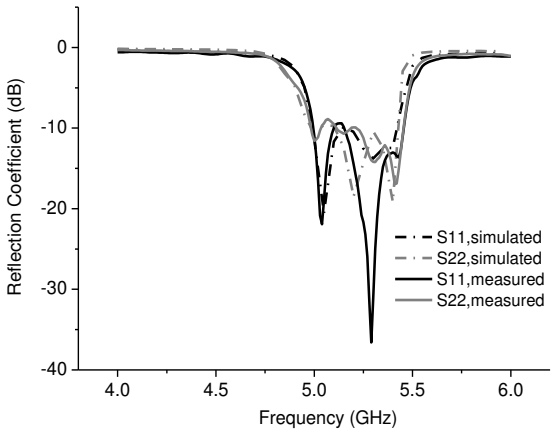

Fig. 16 The simulated and measured S parameters of the SLR-fed array.

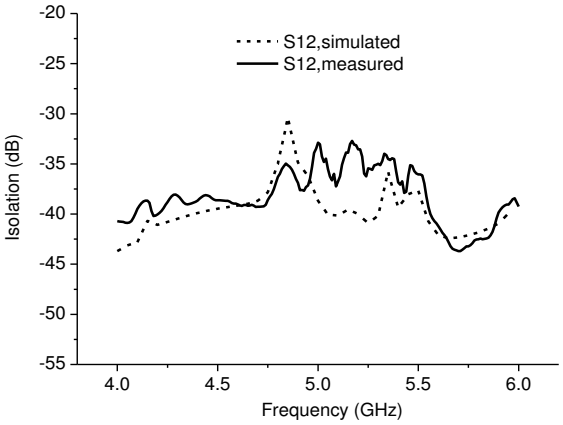

Fig. 17 The simulated and measured isolation between the two ports.

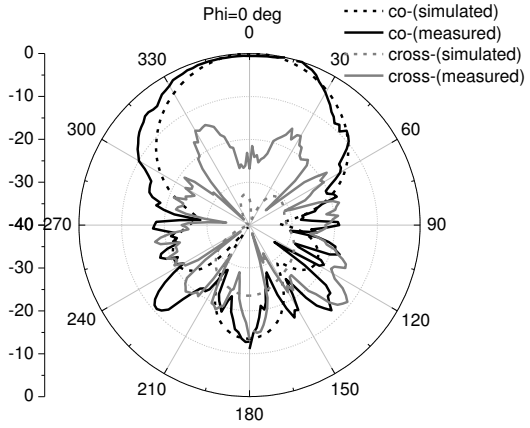

(a) $\varphi=0^0$

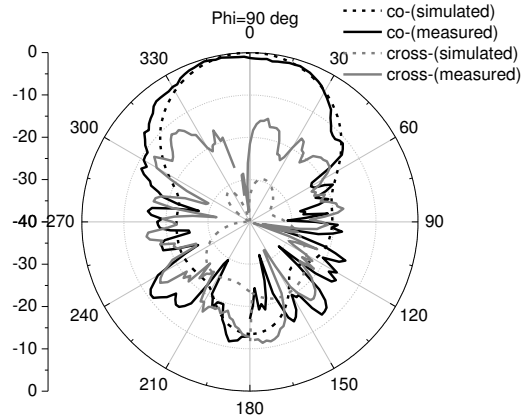

(b) $\varphi=90^0$

Fig. 18 The normalized simulated and measured co- and cross-polarization radiation patterns at 5.2 GHz when port 1 is excited: (a) $\varphi=0^0$, (b) $\varphi=90^0$.

of 470 MHz. What is more, the unmatched bandwidth between the patch array and the filter introduces unexpected degradation of performance due to multiple reflections (as shown at 4.95 GHz). In contrast, for the integrated design proposed in this work, not only the size of subsystem is reduced, but also the bandwidth and frequency selectivity are improved. The much enhanced bandwidth results from the coupling between the narrowband patch and dual-mode filter. In addition, the integrated filter-antenna shows a sharp transition from the operation band to the rejection band. As shown in Fig. 15, at 5.6 GHz, 8 % above the central frequency, the S_{11} is -3 dB for the traditional patch, but only -0.5 dB for the SLR-fed array. The bandwidth is improved significantly from 3.3 % to 9.1 %.

V. RESULTS AND DISCUSSION

The simulated and measured S_{11} and S_{22} of the 2×2 SLR-fed antenna array are presented in Fig. 16. It is observed that measured results agree well with the simulations, showing a broadband performance from 4.96 GHz to 5.48 GHz (fractional bandwidth =10%).Three reflection zeros located at 5, 5.25 and 5.45 GHz can be identified in S_{11} and S_{22}. The results exhibits a high frequency selectivity and out-of-band rejection. The small difference between the simulated and measured results can be attributed to fabrication errors. Fig. 17 shows the simulated and measured isolation between the two ports. The measured isolation is better than 32 dB between the two ports. This indicates the coupling between the SLRs in the two polarizations is weak.

Fig. 18 shows the normalized simulated and measured co- and cross-polarization radiation patterns of the array in two orthogonal planes at 5.2 GHz when port 1 is excited and the port 2 is terminated with a 50 Ω load. The simulated and measured results agree well with each other, exhibiting a maximum radiation in the broadside. The cross polarization discrimination is over 20 dB in XOZ plane ($\varphi=0^0$) and YOZ plane ($\varphi=90^0$).

Fig. 19 shows the simulated and measured normalized radiation patterns in $\varphi=0^0$ and $\varphi=90^0$ planes at 5.2 GHz when port 2 is excited whereas the port 1 is terminated with a 50 Ω load. The antenna exhibits a similarly radiation patterns as port 1 excitation. The main polarization is in y-axis direction with a cross polarization discrimination over 22 dB in the two orthog-

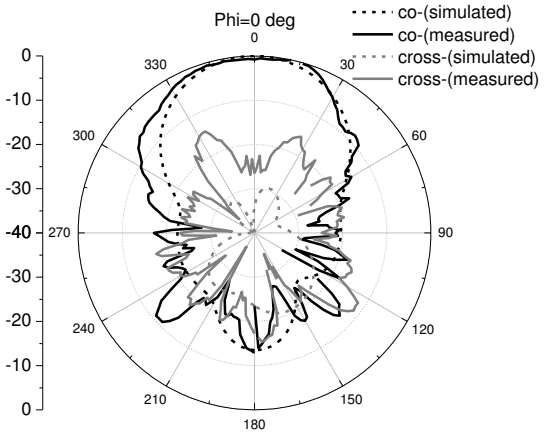

(a) $\varphi = 0^0$

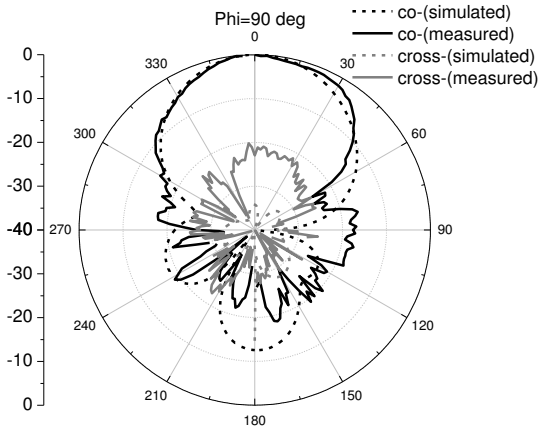

(b) $\varphi = 90^0$

Fig. 19 The normalized simulated and measured co- and cross-polarization radiation patterns at 5.2 GHz when port 2 is excited: (a) $\varphi = 0^0$, (b) $\varphi = 90^0$.

onal planes. It is worth mentioning that the backward radiation patterns show more deviation from the simulation. This is mainly due to a limitation from the measurement system where the rotation joint is directly behind the antenna under test.

The measured antenna gains when two ports are excited independently are shown in Fig. 20. It is observed that the proposed antenna array has a flat antenna gains of about 10.5 dBi from 4.9 to 5.3 GHz. Out of the band, the gains drop rapidly to below -7 dBi at 4.6 and 5.7 GHz. For comparison, the gains of a traditional 2×2 patch array is added. It is observed that the gain of the traditional array is about 12 dBi at 5.2 GHz and decreases slowly when the frequency deviates from the center frequency. In contract, the SLR-fed array exhibits a much higher out-of-band rejection. The measured radiation efficiency are also displayed in Fig. 20. It is over 80% in the operating band. Out of the band, the efficiency drops sharply to 10 % or below above 5.5 GHz and below 4.7 GHz, which is caused by the frequency selectivity of the integrated SLR in the design.

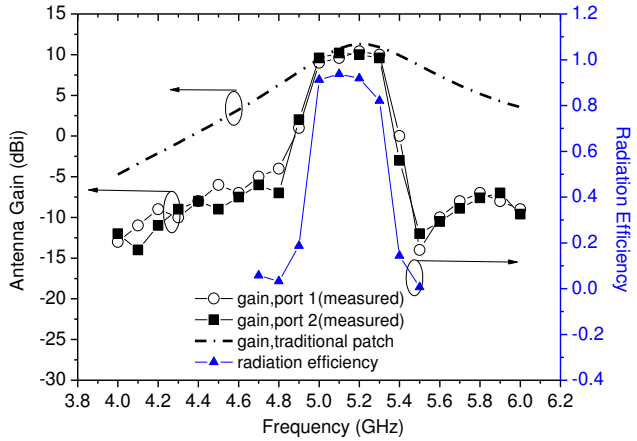

Fig. 20 The measured antenna gain and radiation efficiency.

VI. CONCLUSION

In this paper, a novel design concept is proposed to integrate dual-mode resonator in a low profile patch antenna for improving the bandwidth and frequency selectivity. To verify the design concept, a 2×2 dual polarization SLR-fed antenna array at C-band is designed, fabricated and tested. The realized array achieved a 10% impedance matching bandwidth and much enhanced frequency selectivity. In the proposed design, the coupling coefficient and bandwidth can be controlled. Compared with the traditional cascaded design of a filter and an antenna, this highly integrated design has the advantages of more compact size, wider bandwidth, increased frequency selectivity and flatter gain response. The measurement results have verified the design concept. Such low-profile broadband dual-polarized arrays are useful for space-borne SAR applications. This concept can be extended to larger-size dual-polarized arrays such as 4×4 or 16×16 arrays.

REFERENCES

[1] R. Pokuls, J. Uher and D. M. Pozar, "Dual-Frequency and Dual-Polarization Microstrip Antennas for SAR Application," IEEE Trans. Antennas and Propag., vol. 46, no. 9, pp. 1289-1296, Sep. 1998.

[2] D. M. Pozar, S. D. Targonski, "A Shared-Aperture Dual-Band Dual Polarized Microstrip Array," IEEE Trans. Antennas and Propag., vol. 49, no. 2, pp. 150-157, Feb. 2001.

[3] S. S. Zhong, Z. Sun, L. B. Kong, C. Gao, W. Wang and M. P. Jin, "Tri-Band Dual –Polarization Shared-Aperture Microstrip Array for SAR Applications," IEEE Trans. Antennas and Propag., vol. 60, no. 9, pp. 4157-4165, Sep. 2012.

[4] R. Caso, A. A. Serra, M. R. Pino, P. Nepa and G. Manara, "A Wideband Slot-Coupled Stacked-Patch Array for Wireless Communications," Antenna Wireless Propag. Lett., vol. 9, pp. 986–989, 2010.

[5] K. L. Wong, H. C. Tung, and T. W. Chiou, "Broadband dual-polarized aperture-coupled patch antennas with modified H-shaped coupling slots," IEEE Trans. Antennas Propag., vol. AP-50, no. 2, pp. 188–191, Feb. 2002.

[6] K. L.Wong and T.W. Chiou, "Broadband dual-polarized patch antennas fed by capacitively coupled feed and slot-coupled feed," IEEE Trans. Antennas Propag., vol. AP-50, no. 3, pp. 346–351, Mar. 2002.

[7] S. Gao and A. Sambell, "Low-Cost Dual-Polarized Printed Array with Broad Bandwidth," IEEE Trans. Antennas Propag., vol. 52, no. 12, pp. 3394-3397, Dec. 2004.

[8] S. Gao and A. Sambell, “Dual-Polarized Broad-Band Microstrip Antenna Fed by Proximity Coupling,” IEEE Trans. Antennas Propag., vol. 53, no. 1, pp. 526-530, Jan. 2005.
[9] A. Abbaspour-Tamijani, J. Rizk, and G. Rebeiz, “ Integration of filters and microstrip antennas,” in Proc. IEEE AP-S Int. Symp., pp. 874–877, Jun. 2002.
[10] Y. X. Guo, K. M. Luk, and K. F. Lee, “Broadband dual-polarization patch element for cellular-phone base stations,” IEEE Trans. Antennas Propag., vol. 50, no. 2, pp. 251–253, Feb. 2002.
[11] Y. Qin, S. Gao and A. Sambell, Broadband high-efficiency linearly and circularly-polarized active integrated antennas, IEEE Trans. on Microwave Theory and Techniques, Vol. 54, No. 6, June 2006, pp. 2723-2732, June 2006.
[12] Y. Qin, S. Gao and A. Sambell, Broadband high-efficiency circularly-polarized active antennas and arrays, IEEE Trans. on Microwave Theory and Techniques, Vol. 54, No. 7, pp. 2910-2916, July 2006.
[13] Y. X. Guo, K. M. Luk, and K. F. Lee, “Broadband dual-polarization patch element for cellular-phone base stations,” IEEE Trans. Antennas Propag., vol. 50, no. 2, pp. 251–253, Feb. 2002.
[14] T. L. Nadan, J. P. Coupez, S. Toutain, and C. Person, “Optimization and miniaturization of a filter/antenna multi-function module using a composite ceramic-foam substrate,” in IEEE MTT-S Int. Microw. Symp. Dig, pp. 219–222., Jun. 1999.
[15] C. X. Mao, S. Gao, Z. P. Zheng, Y. Wang, F. Qin, B. Sanz, Q. X. Chu, “Integrated Filtering-Antenna with Controllable Frequency Bandwidth,” in Europe Conf. Antennas and Propag. 2015, accepted to be published.
[16] X. Y. Zhang, J. X. Chen, Q. Xue and S. M. Li, “Dual-band Bandpass Filters Using Stub-Loaded Resonators,” Micro. and Wireless Components Lett., vol. 17, No. 8, pp. 583-585, Aug. 2007.
[17] J. S. Hong and M. J. Lancaster, Microwave Filger for RF/Microwave Application. New York: Wiley, 2001.
[18] C. Y. D. Sim, C. C. Chang, J. S. Row, “Dual-Feed Dual-Polarized Patch Antenna With Low Cross Polarization and High Isolation,” IEEE Trans. Antennas Propag., vol. 57, no. 10, pp. 3321–3324, Oct. 2009.